Journal of Materials Chemistry A

Accepted Manuscript

This article can be cited before page numbers have been issued, to do this please use: L. Merí-Bofí, S. Royuela, F. Zamora, L. Ruiz-Gonzales, J. Segura, R. Muñoz-Olivas and M. J. Mancheño, *J. Mater. Chem. A*, 2017, DOI: 10.1039/C7TA05588A.

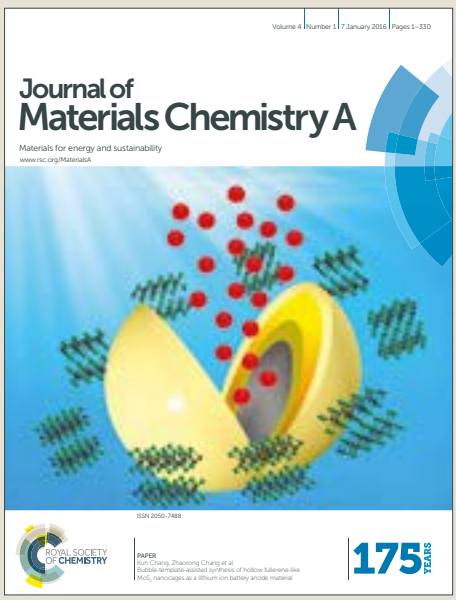

ROYAL SOCIETY OF CHEMISTRY

rsc.li/materials-a

DOI: 10.1039/C7TA05588A

Journal Name

ARTICLE

Thiol Grafted Imine-Based Covalent Organic Framework for Water Remediation Through Selective Removal of Hg(II)

Received 00th January 20xx,
Accepted 00th January 20xx

DOI: 10.1039/x0xx00000x

www.rsc.org/

Laura Merí-Bofí,[a] Sergio Royuela,[a] Félix Zamora,[b] M. Luisa Ruiz-González,[c] José L. Segura,[*a] Riansares Muñoz-Olivas,[*d] María José Mancheño[*a]

An imine-linked covalent organic framework (**[HC≡C]$_{0.5}$-TPB-DMTP-COF**), endowed with reactive ethynyl groups on the walls of one-dimensional pores, has been used as a platform for pore-wall surface engineering with triazole and thiol groups to yield **TPB-DMTP-COF-SH**, which is suitable to interact very efficiently with mercury ions. The evaluation of the carefully designed **TPB-DMTP-COF-SH** is addressed as an effective and selective system for mercury sorption. The obtained results reveal an extraordinary capacity and a great efficiency of the polymeric material with a very high distribution coefficient value $K_d = 3.23 \times 10^9$. Thus, the level of mercury of a highly concentrated aqueous solution, 10 mg L^{-1} of Hg(II), is dramatically decreased, below the limits of what is considered to be drinking water, upon treatment with **TPB-DMTP-COF-SH** for a few minutes. The **TPB-DMTP-COF-SH** retention value of Hg(II) from water is 99.98 % within 2 minutes and its record uptake capacity is 4,395 mg g^{-1} which represents the highest value reported so far. Besides **TPB-DMTP-COF-SH** captures other extremely toxic heavy metal ions such as Sn(II) and Pb(II) being quite selective versus Cd(II) or As(III). These results suggest that **TPB-DMTP-COF-SH** constitutes a realistic alternative for the remediation of contaminated spaces from an environmental perspective.

Introduction

Mercury is one of the most harmful heavy metals due to its high toxicity and bioaccumulation.[1] Mercury pollution can cause a wide range of diseases in human beings and other species. Therefore, it is considered to be a global threat regarding public health and the environment.[2] Since the episode that took place in Minamata (Japan)[3] there have been numerous initiatives on a global scale to restrict the use of this highly toxic element. Nevertheless, nowadays it is still present in consumer products such as drugs or cosmetics, as well as, to a large extent, in various kinds of industrial waste including fossil fuel combustion, batteries and electronic devices.[4] Additionally, metals down to trace levels (e.g. < 5 parts per billion (ppb)) remains a challenge.[5] In this regard, for instance, the Environmental Protection Agency of the United States (EPA) has established an upper limit of 2 ppb for mercury in drinking water[6] and it has also limited the amount of this element to even much lower values for its release into aquatic systems in order to preserve the ecosystems.[7]

Due to its solubility and stability, Hg(II) is the common inorganic form of mercury as pollutant. It is, therefore, necessary to develop efficient systems to capture and detect this toxic element efficiently and selectively. In order to pursue this goal, a lot of effort has been put into the preparation and functionalization of various conventional adsorbent materials to capture and remove Hg(II) from contaminated water,[8] such as activated carbon,[9] zeolites[10] and clays,[11] generally with a low capacity and affinity for mercury. Additionally, novel chemically designed materials such as Metal-Organic Frameworks (MOFs),[12] layered double hydroxides,[13] porous organic polymers (POPs)[14] and MoS_2 nanosheets[15] have been implemented with good results.

In recent years, a new family of polymeric porous and crystalline materials, the so-called Covalent Organic Frameworks (COFs), have emerged.[16] The high surfaces areas, regular porous structure, great adsorption capacity and chemical stability of COFs make these materials appealing as potential candidates for uses as water decontamination agents. COFs can be synthesized *ad-hoc* by a correct choice of molecular blocks and diverse methods, providing different versatile structures. Moreover, it has been proved that such frameworks can be post-functionalized suitably in order to improve or introduce new performances maintaining their crystalline and porous features.[17] Therefore, COFs fulfill all the requirements for the correct design of adsorbent materials for

[a] Departamento de Química Orgánica I, Facultad de CC. Químicas, Universidad Complutense de Madrid, Madrid 28040, Spain.
[b] Departamento de Inorgánica, Facultad de Ciencias, Universidad Autónoma de Madrid, Madrid 28049, Spain.
[c] Departamento de Química Inorgánica, Facultad de CC. Químicas, Universidad Complutense de Madrid, Madrid 28040, Spain.
[d] Departamento de Química Analítica, Facultad de CC. Químicas, Universidad Complutense de Madrid, Madrid 28040, Spain.

Electronic Supplementary Information (ESI) available: See DOI: 10.1039/x0xx00000x

View Article Online
DOI: 10.1039/C7TA05588A

specific contaminant removal from water. Recently, a new hydrazone linked COF was

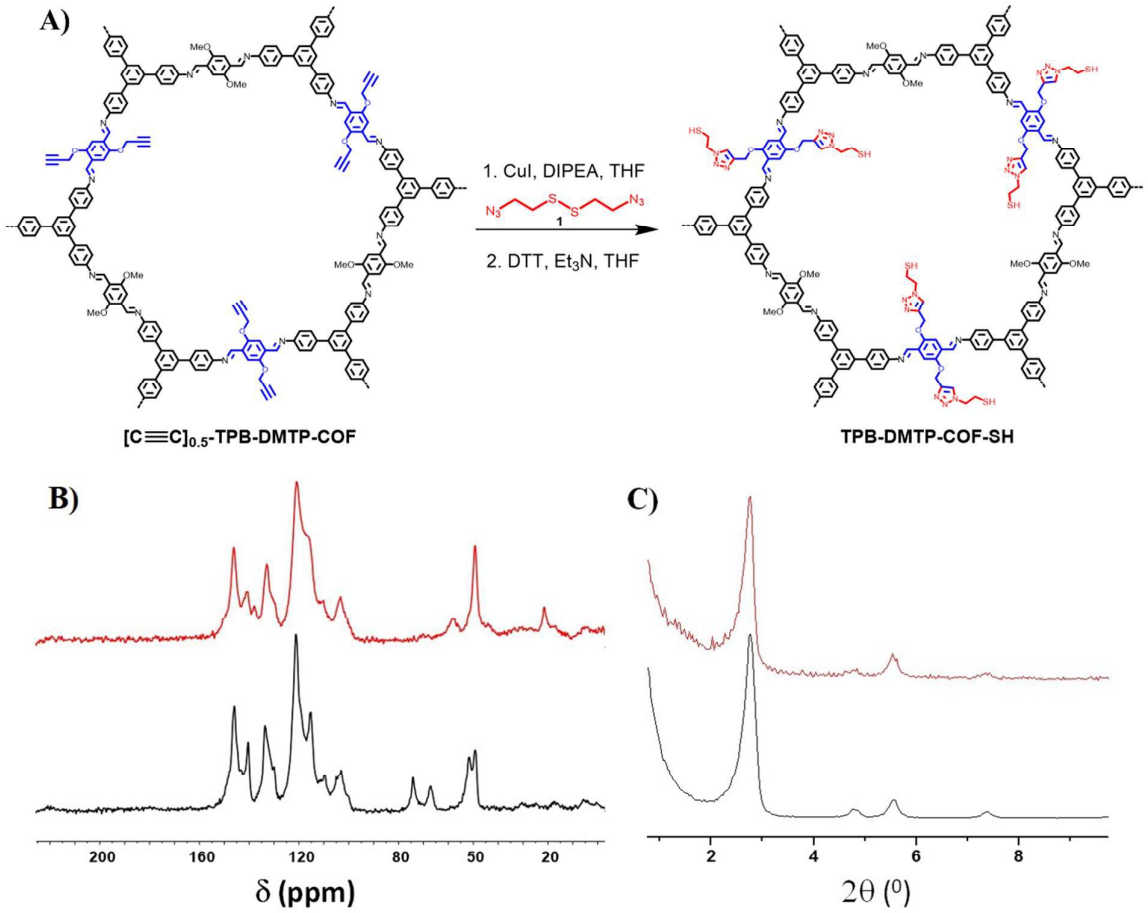

Figure 1. A) Schematic synthesis of **TPB-DMTP-COF-SH**. B) ^{13}C CP/MAS NMR spectra of **[HC≡C]$_{0.5}$-TPB-DMTP-COF** (black line) and **TPB-DMTP-COF-SH** (red line). C) Powder X-ray diffraction patterns of **[HC≡C]$_{0.5}$-TPB-DMTP-COF** (black line) and **TPB-DMTP-COF-SH** (red line).

reported as a high sensitive chemosensor for selective Hg(II) detection, but not efficient enough to act as a competitive sorbent for water decontamination.[18] Finally, it is worth mentioning that parallel to this work Jiang *et al.*[19] and Ma *et al.*[20] have just reported on the first two COFs with good capacities as Hg(II) sorbents.

With the aim of improving the state-of-the-art in relation to the capacity of COFs to adsorb and quantify Hg(II) in environmental samples, we have designed a strategy based on a thermally and chemically stable COF showing high crystallinity, porosity, surface area and easy to synthesize at a large scale, as verified by us in this work. Additionally, the selected COF is suitable for post-functionalization with triazole and thiol groups on flexible arms. The latter feature is very desirable, since it will combine flexibility with the well-known affinity of mercury for sulfur atoms [12b, 19-21] and the high coordinative capacity of triazole ligands towards Hg(II).[22] We expect that this combination leads to a synergistic chelator effect of Hg(II) species. The selected starting COF, named as **[HC≡C]$_x$-TPB-DMTP-COF** (x = 0.17, 0.34, 0.50)[17a] (Figure 1A), fulfills all the requirements mentioned above. The relatively high surface area, regular structure and permanent porosity of these two-dimensional (2D) COFs are good indicators of the potential accessibility of the triazole and thiol groups within the polymeric network to attain the Hg(II) ions. Otherwise, the presence of alkyne groups in the porous framework allows a highly tunable molecular design by direct functionalization in the solid phase by click reactions to introduce both, the triazole and thiol moieties. Finally, the possibility of controlling the quantity of alkynes present in the pore constitutes an excellent approach to modulate the amount of functional groups able to interact with the adsorbate and control its diffusion without blocking the pore.

Therefore, we selected the COF incorporating three alkyne groups *per* pore, named as **[HC≡C]$_{0.5}$-TPB-DMTP-COF**, as the starting precursor to incorporate both triazole and thiol groups by using the well-known "Click Chemistry" based on the copper-catalyzed Huisgen´s 1,3-dipolar cycloaddition of azides and terminal alkynes (CuAAC) (Figure 1A).[23] Triazoles are very useful ligands in coordination chemistry because of their

View Article Online
DOI: 10.1039/C7TA05588A

diverse binding behaviors, depending on the position and nature of the substituents on the triazole ring.[22, 24] Otherwise, well-established mercury–sulfur chemistry is of great interest due to the biological and environmental importance of the metal and, in particular, the structural chemistry of Hg(II) thiolates that affords a great variety of assemblies.[21] Consequently, it was reasonable to consider that the incorporation of triazole moieties combined with well-designed thiols groups could provide suitable channels decorated with flexible arms for mercury removal in a cooperative fashion, somehow mimicking coordination modes of biological systems.[25, 26] Otherwise, **[HC≡C]$_{0.5}$-TPB-DMTP-COF** balances the number of thiol groups in the cavity with the accessibility of metal ions.[20,27] Thus, a precise and rational architecture of the pore contributes to increase the adsorption efficiency of the desired COF. Herein, we show the design, synthesis and characterization of a novel imine-based COF containing triazole and thiol groups located at the cavities with a great capacity of mercury retention. This material shows a benchmark performance to remove and/or immobilize and to determine the presence of Hg(II) in water. In fact, it shows the highest mercury uptake capacity known among thiol and thioether functionalized materials so far.

Results and Discussion

Synthesis and characterization of COFs: As stated above, the synthesis of the new COF was accomplished by a two-step reaction sequence from **[HC≡C]$_{0.5}$-TPB-DMTP-COF**[17a] and 1,2-bis(2-azidoethyl)disulfane **1**[28] (Figure 1A). A challenging matter in the development of sorbents for practical applications is a large-scale synthesis in a sustainable way. Therefore, we first carried out a larger-scale preparation of the starting COF, **[HC≡C]$_{0.5}$-TPB-DMTP-COF** (1:20 fold with respect to the previously reported reaction scale, see SI for details). The **[HC≡C]$_{0.5}$-TPB-DMTP-COF** was characterized by Fourier transform infrared spectroscoy (FTIR) (Figure S1), ^{13}C cross-polarized magic angle spinning solid-state NMR (^{13}C CP/MAS NMR) (Figure 1B) and UV-vis spectroscopy (Figure S3). Additionally we measured its powder X-ray diffraction (PXRD) (Figures 1C and S2; Tables S1 and S2) and Brunauer–Emmett–Teller (BET) surface area, pore volume and pore size derived from nitrogen sorption isotherms (Figure 2, Table S5). These characterization data are in good agreement with those previously reported.[17a]

The incorporation of thiol groups into the COF was accomplished by reaction of bisazide **1** with [**HC≡C]$_{0.5}$-TPB-DMTP-COF** in a mixture of THF/H_2O in the presence of *N,N*-diisopropylethylamine (DIPEA), CuI and toluene, yielding a brown solid insoluble in the mixture. The solid obtained was further treated with the Clealand reagent (Dithiothreitol, DTT), giving rise to a brown solid, **TPB-DMTP-COF-SH** (Figure 1A). Remarkably, this method prevents the easily oxidation of the thiol group as it is already incorporated by *in situ* reduction of the disulfide groups in the inner core of the COF, it is performed under mild conditions and could be implemented at large scale. Thus, the material may be stored and readily reduced before its use. **TPB-DMTP-COF-SH** was characterized by FTIR, ^{13}C CP/MAS NMR and UV-vis spectroscopies. Interestingly, the FTIR spectrum of **TPB-DMTP-COF-SH** does not show the characteristic azide peak at 2101 cm^{-1}, suggesting the complete incorporation of the thiol group (Figure S4), while the S-H stretch appears at 2590 cm^{-1} (Figure S36). Additionally, the **TPB-DMTP-COF-SH** ^{13}C CP/MAS NMR spectrum shows the signals corresponding to the *C*sp^2 between 105-160 ppm, an intense signal at 54.4 ppm assignable to the methoxy groups and less intense signals at 63.7, 48.5 and 25.7 ppm corresponding to the *C*H$_2$ groups of the aliphatic chains that are grafting the thiol group into the covalent network (Figure 1B). The almost quantitative post-synthetic reaction is confirmed by the disappearance of the *C*sp signals at 80 and 73 ppm and the O*C*H$_2$ signal of the alkynyl fragment at 56 ppm (Figure 1B). Moreover, Energy-dispersive X-ray spectroscopy (EDS) (Figure S20) and elemental analysis support a correct functionalization of the pristine channels. **TPB-DMTP-COF-SH** was also characterized by scanning electron microscopy (SEM) showing a laminar structure (Figures S23) with a homogenous composition (Figures S21 and S22). High resolucion transmision electron microscopy (HRTEM) of **TPB-DMTP-COF-SH** confirms the laminar structure being in agreement with the XRD data and porosity information (Figure S27 and Table S5). Finally, the UV-vis spectra of both **[HC≡C]$_{0.5}$-TPB-DMTP-COF** and **TPB-DMTP-COF-SH** exhibit a nearly identical profile (Figure S3) indicating that the conjugated skeleton in the network remains unaltered after the reaction.

Porosity: The porosity of **TPB-DMTP-COF-SH** was investigated evaluating its nitrogen sorption isotherm at 77 K. The sorption curve consists of a typical type IV isotherm (Figure 2) characteristic of mesoporous materials. The BET (Brunauer, Emmett and Teller) surface area and pore volume were estimated to be 291 m^2 g^{-1} and 0.41 cm^3 g^{-1}, respectively. The pore size distribution calculated by using the non-local density functional theory (NLDFT) method resulted in a pore size of 2.14 nm.

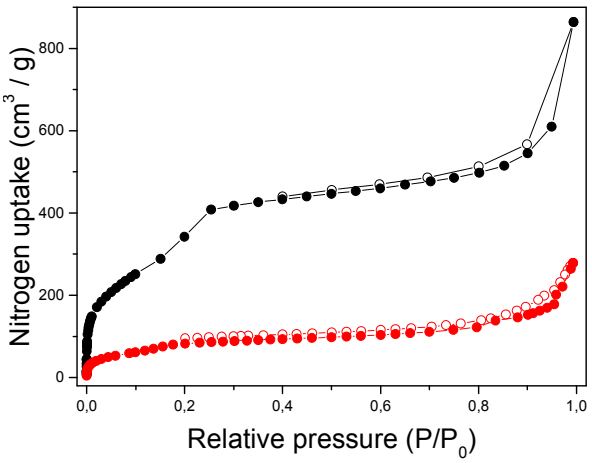

Figure 2. Comparison of nitrogen adsorption isotherms of **[HC≡C]$_{0.5}$-TPB-DMTP-COF** (black) and **TPB-DMTP-COF-SH** (red).

Adsorption capability: The capability of **TPB-DMTP-COF-SH** to capture Hg(II) ions from aqueous solutions has been evaluated using a Direct Mercury Analyzer (DMA-80). On a typical experiment, a solid sample of **TPB-DMTP-COF-SH** (19.7 mg)

View Article Online
DOI: 10.1039/C7TA05588A

was placed in a 1 mL aqueous solution (pH of 5.6) of $HgCl_2$ with Hg(II) concentration of 10 mg L^{-1}. Then, the suspension was stirred for 10 min at 24 °C and the solid filtered-off, named as **TPB-DMTP-COF-SHg**. EDS spectrum (Figure S20) and SEM images (Figure 3) of **TPB-DMTP-COF-SHg** confirm the presence of mercury (see also S25-S26 for mapping). Furthermore, the absence of the characteristic S–H stretching mode at 2590 cm^{-1} in the FTIR spectrum of **TPB-DMTP-COF-SHg** verifies the coordination of the thiol groups to Hg(II) (Figure S36).

The mercury removal from water by **TPB-DMTP-COF-SH** is very fast. Thus, only 10 min after the addition of **TPB-DMTP-COF-SH**, the Hg(II) concentration in the solution decreases to 1.5 μg L^{-1}. Therefore, a mercury removal efficiency from water of *ca*. 99.98 % is observed. Interestingly, an experiment carried out under similar experimental conditions, but using a higher V/m_{COF} ratio of 1,976 mL g^{-1}, also showed a very fast mercury removal from water, reaching up to 98.23 % in just 2.5 min, and quantitative mercury uptake (99.99 %) within 2 h.

The **TPB-DMTP-COF-SH** sorbent's affinity for Hg(II) was estimated by the distribution coefficient (K_d) measurement. The K_d is defined as:

$$K_d = \frac{(C_i - C_f)}{C_f} x \frac{V}{m} \qquad (1)$$

where C_i is the initial metal ion concentration, C_f is the final equilibrium metal ion concentration, V (mL) is the volume of the treated solution and m (g) is the mass of sorbent used. A K_d value of 3.23×10^5 mL g^{-1} was obtained for the 10 mg L^{-1} Hg(II) sample after only 10 min, indicating a very high adsorption capacity. Longer times (up to 2h) gave rise to K_d values up to 3.23×10^9 mL g^{-1}, calculated for a sample of 25.3 mg COF/50 mL of 10 mg L^{-1} of Hg(II) (V/m_{COF} = 1,976 mL g^{-1}). Indeed, this is a much higher value than the benchmark thiol-sorbents COF-S-SH,[20] $K_d = 2.3 \times 10^9$ mL g^{-1} (25 mg COF-S-SH/50 mL of 10 mg L^{-1} of Hg(II), V/m = 2,000 mL g^{-1}, contact time: 12 h), PAF-SH,[14a] $K_d = 5.76 \times 10^7$ mL g^{-1} (25 mg PAF-SH/50 mL of 10 mg L^{-1} of Hg(II), V/m = 2,000 mL g^{-1}, contact time: 4 h) or other recently described sorbents such as MoS_2 nanosheets,[15] $K_d = 3.53 \times 10^8$ mL g^{-1} (10 mg MoS_2 / 100 mL of 10 mg L^{-1} of Hg(II), V/m = 10,000 mL g^{-1} contact time: 24 h), MoS_4-LDH,[13] $K_d = 1.1 \times 10^7$ mL g^{-1} (30 mg MoS_4-LDH / 30 mL of 10 mg L^{-1} of Hg(II), V/m = 1,000 mL g^{-1}, contact time: 6 h), TAPB-BMTTPA-COF,[19] $K_d = 7.82 \times 10^5$ mL g^{-1} (25 mg TAPB-BMTTPA-COF/50 mL of 10 mg L^{-1} of Hg(II), V/m = 2,000 mL g^{-1}, contact time: 12 h).

Therefore, **TPB-DMTP-COF-SH** is in the range of the best sorbent materials so far reported, even better than some of the commercial ones including resins (K_d ~10–5.1×10^5 mL g^{-1}),[29] silane chelating fibers ($K_d = 3.0 \times 10^5$–3.8×10^6 mL g-1),[30] Chalcogel-1 ($K_d = 9.2 \times 10^6$–1.6×10^7 mL g^{-1})[31] and thiol-functionalized silicates ($K_d = 3.4 \times 10^5$–1.0×10^8 mL g^{-1}).[32]

PXRD measurements were carried out after mercury removal experiments, in order to evaluate the robustness to the experimental conditions and the structural effects of the mercury incorporation to the **TPB-DMTP-COF-SH**. The diffraction patterns show that all the samples retain their crystalline structure confirming both chemical stability and little structural effects of mercury incorporation into the cavities (Figure S16, Tables S9 and S10).

Few examples of metal ions incorporated into COFs have still been reported.[33] Interestingly, it is known that linking of palladium to an imine-based COF caused a high structural distortion with a significant effect on its diffractogram.[33] Our result suggests that the metal-thiol or triazole interactions, instead of metal-*N*-imine, is more suitable for mercury ion incorporation into the COF structure without significant network distortion, even when mercury is much larger than palladium.

Finally, SEM images of **TPB-DMTP-COF-SH** samples treated with Hg(II) confirm that their morphology is unaltered upon mercury incorporation (Figure 3, see also Figures S23-S26).

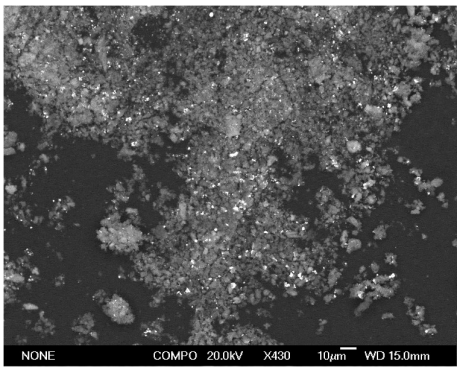

Figure 3. SEM image by retrodispersion of **TPB-DMTP-COF-SHg**.

Effect of sorbent dosage: Similar batch experiments were carried out by mixing a solution of 1 mL of a highly concentrated sample of Hg(II) (10 ppm) with different quantities of **TPB-DMTP-COF-SH**, (2.5, 5, 7,5, 10, 12.5, 15, 20 mg) to evaluate this parameter. The mixture, in each case, was shaken for 10 min, the pristine was filtered off, washed with water and the Hg(II) concentration was measured in the extracts as usual. (see SI, table S13). For all cases, adsorption is observed. For the small dose of 2.5 mg only a 40% of retention was obtained being almost quantitative for the 20 mg dose.

Adsorption Kinetics: Concentrated mercury contaminated water solutions have been used to determine the kinetics of the heavy metal adsorption by **TPB-DMTP-COF-SH**, using Hg(II) solutions at different ratios of V(mL)/m_{COF} (mg). Thus, firstly 1 mL of aqueous 10 mg L^{-1} $HgCl_2$ at pH = 5.6 was treated with 19.7 mg of **TPB-DMTP-COF-SH**. Extremely fast kinetic was observed. Mercury removal reaches up to 99.98 % of mercury adsorption capacity at equilibrium within 2 min. On the other hand, when a sample of contaminated water with a concentration of 7.4 mg L^{-1} of $HgCl_2$ is treated with **TPB-DMTP-COF-SH** (V/m ratio 1,976 mL g^{-1}), the adsorption is slower reaching only 97.23 % in 10 min, but it is almost completed within 2 h (99.99 %, Table S7).

Different kinetic models have been developed to describe the kinetics of heavy metal removal.[34] In this case, the data are very well fitted by the pseudo-second order model, expressed as equation 2:

View Article Online
DOI: 10.1039/C7TA05588A

$$\frac{t}{q_t} = \frac{1}{k_2 q_e^2} + \frac{t}{q_e} \qquad (2)$$

where k_2 (g mg^{-1} min^{-1}) is the rate constant of pseudo-second order adsorption, q_t (mg g^{-1}) is the amount of Hg(II) adsorbed at time t (min), and q_e (mg g^{-1}) is the amount of Hg(II) adsorbed at equilibrium.

For the Hg(II) adsorption data a fast kinetic adsorption process with k_2 = 11.5 g mg^{-1} min^{-1} and an extremely high correlation coefficient (R^2 = 1) is observed (Figures 4A, S14 and Table S8). As a result, **TPB-DMTP-COF-SH** is more efficient than the best thiol grafted material so far reported, PAF-SH[14a] (k_2 = 8.13 *vs* k_2 = 11.5 obtained under similar conditions), and better than the thio-functionalized COF recently reported as mercury sorbent, TAPB-BMTTPA-COF[19] (k_2 = 6.31; data obtained under similar conditions).

Hg(II) Uptake: To assess the mercury uptake capacity of **TPB-DMTP-COF-SH**, the adsorption isotherm for Hg(II) removal from water (initial pH of 5.6) was collected at 24 °C (SI for experimental details, Table S11). The experiment was carried out under similar experimental conditions to those used for K_d determination, but the mercury concentrations were progressively increased from an initial concentration of 500 µg L^{-1} until saturation of the sample. Measurements were duplicated to ensure reproducibility showing similar results. The points were well-fitted with Langmuir and Freundlich models[35] yielding high correlation coefficients (Figure S17) but the data are better fitted by the Langmuir model (R^2 = 0.998), suggesting a monolayer adsorption (Figure 4B).

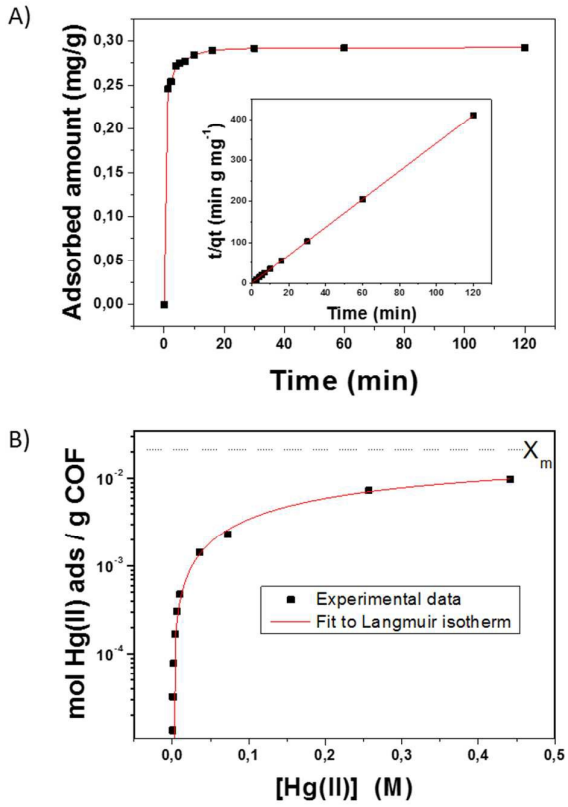

Figure 4. A) Kinetics investigation of **TPB-DMTP-COF-SH**. Hg(II) sorption under Hg(II) initial concentration of 7.4 mg L^{-1} (m_{COF} = 25.3 mg/V = 50 mL). Inset shows the pseudo-second-order kinetic plot for the adsorption. B) Inset of Langmuir isotherm (X_m is the theoretical maximum sorption capacity).

The Langmuir isotherm model is listed as:

$$x/x_m = K\,c/\,1 + K\,c \qquad (3)$$

where c is the Hg(II) concentration at equilibrium, x is the adsorbed Hg(II) amount for that concentration, and K and x_m are the Langmuir constants that represent the affinity constant and the theoretical maximum sorption capacity respectively. Thus, a value of K = 1.87 L mol^{-1} and a saturation uptake capacity of 0.021 mol g^{-1} (4,395 mg g^{-1}) are obtained. These results are excellent in comparison to the recently reported best Hg(II) thiol-sorbent COF-S-SH (1,350 mg g^{-1}).[20] It is also better than PAF-1-SH (1,014 mg g^{-1})[14a] and other thio-functionalized sorbents as MoS_2 nanosheets (2,506 mg g^{-1}),[15] mesoporous silica (505-600 mg g^{-1}),[27c,33b] thiopyrene-featured porous carbon (518 mg g^{-1}),[27e] Chalcogel-1 (645 mg g^{-1}),[31a] MoS_4^{2-} intercalated LDH (500 mg g^{-1}),[13] MOF FJI-H12 (439.8 mg g^{-1})[12a] and TAPB-BMTTPA-COF (734 mg g^{-1}).[19] (Figure 5).

View Article Online
DOI: 10.1039/C7TA05588A

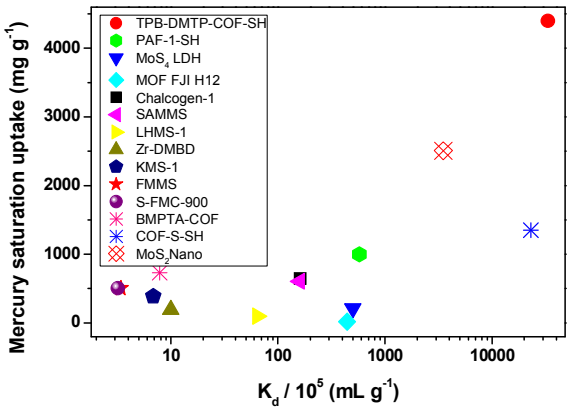

Figure 5. Comparative of the maximum retention capacity of Hg(II) and K_d of some benchmark materials under similar conditions: KMS-1,[36] LHMS-1,[37] FMMS,[27c] Chalcogel-1,[31a] S-FMC-900,[27e] Zr-DMBD,[12b] SAMMS,[29a] PAF-1-SH,[14a] MoS_4-LDH,[13] FJI-H12,[12a] MoS_2 nanosheets,[15] TAPB-BMTTPA-COF,[19] COF-S-SH,[20] TPB-DMTP-COF-SH (this work).

The outstanding saturation mercury uptake capacity (Figures 4B and 5) can be attributed to a high metal ion surface area together with the well-designed **TPB-DMTP-COF-SH** cavity (Figure 1A) with the appropriate amount of triazole and thiol groups that are accessible throughout the inner surface. Other aspect that can benefit the high adsorption is the nanometric size of the COF particles; in fact nanoparticles play an important role in adsorption-desorption of heavy metals because of small sizes and high surface area.[14a]

Hg(II) Uptake as a function of pH: For practical use, removal of Hg(II) under harsh conditions, such as extreme pH values, is desired. Thus, the chemical stability and adsorption capacity of **TPB-DMTP-COF-SH** was comparatively tested at different pHs (pH = 2, 5.4 and 12 respectively, 20 mg COF/50 mL of 10 mg L^{-1} Hg(II) solution, 10 min). A similar high removal efficiency for the samples in the range of pH 5.4-12 was observed and crystallinity of **TPB-DMTP-COF-SH** was also maintained throughout all the experiments. However, for the sample loaded at pH = 2, we observed less retention capacity with appreciable leaching after loading. This behavior is in accordance with the adsorption of Hg(II) observed in other sulfur-functionalized carbon materials at low pH, in which the positively charged carbon surface and the also positively charged mercury complex (like $S\text{-}Hg^{+}$ or Hg^{2+}) may act as electrostatic barrier and prohibit further adsorption.[38] In contrast, the samples treated in the pH range 5-12, remained unaltered, even after successively washing the COF samples with an acid water solution (pH = 1.9). This is an important feature because a highly basic Hg(II) industrial waste (pH = 10) is produced by the chlor-alkali manufacturing industry, being one of the main sources of Hg(II) water pollution, and the pristine is extremely efficient in this medium.[39]

Recycling: Recycling tests were performed on **TPB-DMTP-COF-SHg** to test its potential reusability by releasing the captured Hg(II). Upon rinsing with water solutions of dithiothreitol with different concentrations (SI for details), a leaching of only 12 % of Hg(II) was observed. However, using a 6 M HCl solution, Hg(II) could be efficiently removed from the material. Successive experiments showed that after four cycles the retention capacity was maintained almost constant (Table S17) while its crystallinity was slightly affected. The BET surface area and pore volume were again calculated for the recycled COF being the former slightly lower than the as-synthesized COF material (265 m^2 g^{-1}). Otherwise, pore volume was maintained. These results may be indicative of the stability of **TPB-DMTP-COF-SHg**, since it is necessary to use harsh conditions to remove Hg(II) from the pristine. Additionaly, Hg(II) is also retained under basic conditions, without leaching.

Selectivity tests: The interefering effect of metal ions is another important factor in the process of metal capacity determination using sorbent materials. Thus, a competitive experiment to determine the Hg(II) adsorbed in the presence of other highly toxic metal ions was firstly tested. A solution containing an equimolar mixture (1 mg L^{-1}) of As(III), Cd(II), Pb(II), Sn(II) and Hg(II) was treated for 10 min with **TPB-DMTP-COF-SH**, filtered and the extracted analyzed. As it is depicted in Figure 6A, **TPB-DMTP-COF-SH** is able to adsorb Hg(II) almost quantitatively in the presence of the other concomitant ions such as Pb(II) or As(III). Subsequently, the effect of the major coexisting ions in real samples such as Na(I), K(I), Mg(II), and Ca(II) on Hg(II) sorption capacity was studied and evaluated using a highly concentrated solution of Cu(II), Ca(II), Mg(II), Zn(II) and Na(I) (100 mg L^{-1}) vs Hg(II) ions (1 mg L^{-1}) (Figure 6B, SI for experimental details, Tables S20, S21). Notably, **TPB-DMTP-COF-SH** can effectively adsorb Hg(II), in only 10 min, even in the presence of high concentrations of the coexisting background ions present in natural water. Finally, breakthrough experiments were performed on a real matrix, seawater (obtained from the Mediterranean Sea, Benidorm, Spain, pH = 7.8). **TPB-DMTP-COF-SH** showed again a quantitative Hg(II) retention and also a great selectivity. (See SI, Figure S30).

The results clearly point out to the differences in the affinity of these ions for competing on the main sorption sites, thiol and triazole groups. The pristine mainly owes its removal ability to its porosity and strong binding affinity of heavy metal ions rationalized through the hard-soft acid and base (HSAB) theory. These behaviours are mainlly influence by the diffence in their charge and size of the hydrated ions, as well as the nature of the porous-loaded functional groups present in the sorbent. Mercury is considered a soft metal, with a particularly high affinity for inorganic and organic reduced sulfur (sulfide and thiol, respectively) ligands. Therefore, thiophilic Hg(II) presents the higher affinity in all the experiments tested being quite selective even in seawater. Only other soft big size metals as Sn(II) or Pb(II) can be competitive in some extent.

View Article Online
DOI: 10.1039/C7TA05588A

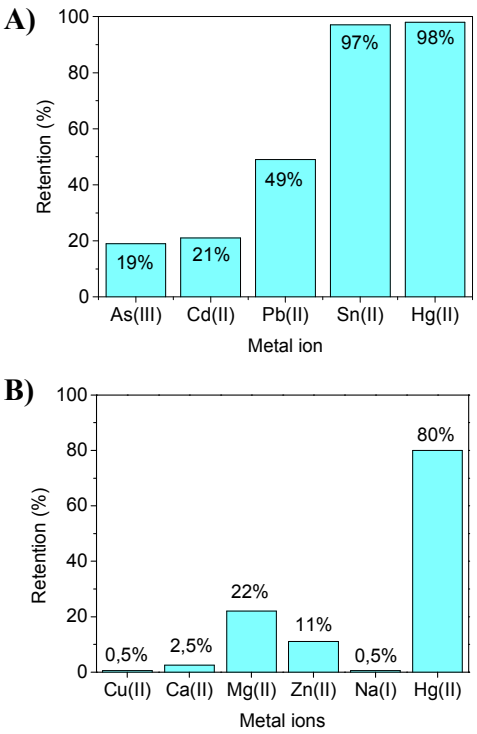

Figure 6. Adsorption selectivity test of **TPB-DMTP-COF-SH** in the presence of other ions: A) As(III), Cd(II), Pb(II), Sn(II), Hg(II) (equimolar concentration, 1 mg.L^{-1}). B) Cu(II), Ca(II), Mg(II), Zn(II), Na(I) (100 mg.L^{-1}) and Hg(II) (1 mg.L^{-1}).

Adsorption mechanism: **TPB-DMTP-COF-SH** shows a superior sorption than that exhibited by the state-of-the-art thiol and/or thioether functionalized adsorbents. Therefore, the co-existence in the cavity of both the thiol and triazole functional groups seems to be determining for the enhancement of Hg(II) adsorption capacity. This was also verified next by comparison of the adsorption behavior of analogous porous COFs. Thus, unfunctionalized sulfur-free COF, **TPB-DMTP-COF**[17a] (Figure S19) gives an uptake of 14 % of Hg(II) *vs* 96 % of **TPB-DMTP-COF-SH** under the same conditions. This result indicates that the imine donors in the COF materials hardly contribute to the capture of Hg(II). Similarly, in order to investigate the role of the triazole moiety on the coordination to Hg(II), **TPB-DMTP-COF-TAZ** (Scheme S3) was also synthesized by treatment of **[HC≡C]$_{0.5}$-TPB-DMTP-COF** with 1-azidopropane (SI for details on preparation and characterization). Its Hg(II) adsorption behavior was tested observing an uptake of 50.4 % *vs* 97 % of **TPB-DMTP-COF-SH** under the same conditions. Therefore, the triazole moiety also has a prominent role in the outstanding sorbent efficiency of **TPB-DMTP-COF-SH**.

Furthermore, binding thiol-Hg(II) interaction is strongly supported by the observed change in the pH value after saturation. The extracted samples increased their acidity from the initial pH = 5.6 to the final pH = 2.2 (after saturation), clearly indicating the release of H^+ ions and the probable exchange of Hg(II) ions with H^+ ions during mercury uptake. Moreover, as stated before, coordination to Hg(II) can also be carried out through triazole moieties, enhancing the adsorption capacity of the pristine. The proper and flexible chelating arms of **TPB-DMTP-COF-SH** can also be arranged in different conformations to appropriately coordinate to Hg(II)[20, 26] in a synergetic way between the triazole and thiol groups.

To get insight into the binding mechanism for this highly effective capture of Hg(II), X-ray photoelectron spectroscopy (XPS) experiments were performed. Mercury inclusion within the pristines **TPB-DMTP-COF-SH** and **TPB-DMTP-COF-TAZ** was confirmed by the appearance of Hg(II) XPS signals at 101.4 and 105.4 eV assigned to the Hg $4f_{7/2}$ and Hg $4f_{5/2}$, respectively (see SI, Figure S31). The binding between Hg(II) and S species in **TPB-DMTP-COF-SHg** was established from the S 2p XPS spectra, which showed a 0.3 eV shift for the S binding energy compared to that in **TPB-DMTP-COF-SH** (163.6 eV) (Figure 7). The XPS signal at 532.0 eV assigned to the O 1s in **TPB-DMTP-COF-SH** is shifted to 532.4 eV in **TPB-DMTP-COF-SHg** and 532.2 eV in **TPB-DMTP-COF-TAZHg.** N 1s is also shifted 0.1 eV in the starting COF **TPB-DMTP-COF-SH** (399.3 eV) in comparison with those at **TPB-DMTP-COF-SHg** and **TPB-DMTP-COF-TAZHg** (399.4 eV). (Figure S32). Therefore, these results allow us to suggest a probable coordination of the Hg(II) to the ether functionality, maybe in a cooperative way with the triazole moiety. Similar coordination environments have been previously described in some triazole derivatives.[40]

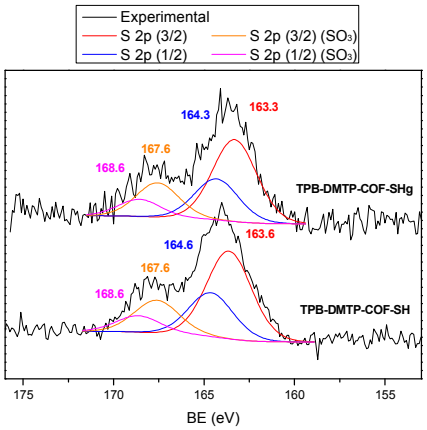

Figure 7. Comparison of the S 2p XPS spectra of **TPB-DMTP-COF-SH** and **TPB-DMTP-COF-SHg.** (The presence of signals at Higher BE values may be adscribed to parcial oxidation of the thiol groups on the surface)

Finally, we also used ^{13}C CP/MAS NMR to evaluate the interaction between Hg(II) and **TPB-DMTP-COF-SH**. Comparison of ^{13}C CP/MAS NMR spectra of **TPB-DMTP-COF-SH** and **TBP-DMTP-COF-SHg** (Figure S35) shows a significant downfield of the signal corresponding to the -CH_2SH, due to coordination to Hg(II) (26 *vs* 35 ppm, respectively) and a slightly broadening in the aromatic region around 149 nm. Thus, it may confirm that the conjugated COF host is able to interact with Hg(II) by a Hg(II)-π interaction. As expected, the imine groups remain unaltered. Similarly, the adsorption behavior was also evaluated by UV-vis spectroscopy. Solids **TPB-DMTP-COF-SH** and **TPB-DMTP-COF-TAZ** exhibit an adsorption band with a maximum at 400 nm (Figure S7). After adsorption of Hg(II), both COFs exhibit the same broad bands with an increased adsorption of the shoulders around 540 nm (Figures S7 and S8), which may be due to the charge transfer from the electron-rich thiol or triazole groups to electron-deficient Hg(II) metal ions.

View Article Online
DOI: 10.1039/C7TA05588A

Conclusions

The extraordinary capacity of a well-designed Covalent Organic Framework which shows triazole and thiol groups located in its cavities as sorbent material for toxic metal ions has been demonstrated. It shows a superior uptake in the state-of-the-art of thiol and/or thioether functionalized adsorbents. The cooperative triazole and accessible thiol (−SH) functions have been incorporated in mild conditions into a highly porous organic polymer **TPB-DMTP-COF** with good yield. This new material captures Hg(II) ranging from trace levels to highly concentrated solutions with outstanding efficiency. The material shows a record saturation mercury uptake capacity and can effectively reduce the Hg(II) concentration from 10 mg L^{-1} to the extremely low level of 1.5 μg L^{-1} in only 10 minutes, which is below the acceptable limits in drinking water standards (2 μg L^{-1}). Thus, **TPB-DMTP-COF-SH** exhibits very high affinity for Hg(II) with exceptional fast kinetics. In addition, **TPB-DMTP-COF-SH** is also effective for mercury removal in presence of high concentrations of background metal ions such as Na(I), Ca(II), Cu(II), Mg(II) or Zn(II) and in real media as seawater. Besides, **TPB-DMTP-COF-SH** captures other extremely toxic heavy metal ions such as Sn(II) and Pb(II) being quite selective *versus* Cd(II) or As(III). These remarkable results offer new perspectives for the use of imine based COFs for decontaminating aqueous media and environmental remediation, a matter of great importance for populations at risk due to mercury pollution, especially in underdeveloped areas.

Conflict of interest

The authors declare no conflict of interest

Acknowledgements

L. M-B and S. R. contributed equally to this work. This work was financially supported by MINECO (MAT2014-52305-P and MAT2016-77608-C3-1-P and 2-P), the CAM (Project S2013/ABI-3028, AVANSECAL-CM) and UCM-BSCH joint project (GR3/14-910759). The authors thank for technical and human support provided by SGIker of UPV/EHU and European funding (ERDF and ESF). This paper is dedicated to Carmen Cámara on occasion of her retirement.

Notes and references

‡ ESI include experimental procedures and characterization data for all compounds. Synthesis, NMR and FTIR spectra, UV-vis, TGA, PXRD profiles, SEM and TEM imaged, EDS, Hg(II) measurements and XPS spectra.

1 M. McNut, *Science*, 2013, **341**, 1430.
2 D. Malakoff, *Science*, 2013, **341**, 1442-1443.
3 S. Ekino, M. Susa, T. Ninomiya, K. Imamura, T. J. Kitamura, *Neurol. Sci.* 2007, **262***,* 131-144.
4 N. Lubick, D. Malakoff, *Science*, 2013, **341**, 1443-1445.
5 K. G. Bhattacharyya, S. S. Gupta, *Sep. Purif. Technol*., 2006, **50**, 388-397.
6 (a) Basic Information about mercury (inorganic) in drinking water.http://water.epa.gov/drink/contaminants/basicinformation/mercury.cfm#four. (b) World Health Organisation, Guidelines for Drinking-Water Quality, Fourth Edition, 2011
7 United States Environmental Protection Agency (EPA). "Treatment technologies for mercury in soil, waste, and water; EPA" Report EPA-542-R-07-003 (U.S. EPA, 2007).
8 (a) D. A. Atwood, M. K. Zaman, *Struct. Bonding*, 2006, **120**, 163-182. (b) S. Ahmed, J. Brockgreitens, K. Xu, A. Abbas *Adv. Funct. Mater.,* 2017, 1606572, DOI: 10.1002/adfm.201606572 and references therein
9 C. P. Huang, D. Blankenship, *Water Res.*, 1984, **18**, 37-46.
10 G. Blanchard, M. Maunaye, G. Martin, *Water Res.*, 1984, **18**, 1501-1507.
11 A. Benhammou, A. Yaacoubi, L. Nibou, B. Tanouti, *J. Colloid. Interface Sci*., 2005, **282**, 320-326.
12 (a) L. Liang, Q. Chen, F. Jiang, D. Yuan, J. Qian G. Lv, H. Xue, L. Liu, H-L. Jiang, M. Hong, *J. Mater. Chem. A*, 2016, **4**, 15370-15374; (b) M. Mon, F. Lloret, J. Ferrando-Soria, C. Martí-Gastaldo, D. Armentano, E. Pardo, *Angew. Chem. Int. Ed*., 2016, **55**, 11167-11172; (c) C. W. Abney, J. C. Gilhula, K. Lu, W. Lin, *Adv. Mater*, 2014, **26**, 7993-7997; (d) K. K. Yee, N. Reimer, J. Liu, S. Y. Cheng, S. M. Yiu, J. Weber, N. Stock, Z. Xu, *J. Am. Chem. Soc*., 2013, **135**, 7795-7998; (e) J. He, K.-K. Yee, Z. Xu, M. Zeller, A. D. Hunter, S. S. Y. Chui, C.-M. Che, *Chem. Mater.* 2011, **23,** 294-298; (f) Q. R. Fang, D. -Q. Yuan, J. Sculley, J. R. Li, Z. B. Han, H. C. Zhou, *Inorg. Chem.,* 2010, **49**, 11637-11642.
13 L. Ma, Q. Wang, S. M. Islam, Y. Liu, S. Ma, M. G. Kanatzidis, *J. Am. Chem. Soc.* 2016, **138**, 2858-2866 and references therein.
14 (a) B. Li, Y. Zhang, D. Ma, Z. Shi, S. Ma, *Nat. Commun.,* 2014, **5**, 5537 and references therein; (b) N. Salamun, S. Triwahyono, A. A. Jalil, Z. A. Majid, Z.; Ghazali, N. A. F. Othman, D. Prasetyoko, *RSC Adv.*, 2016, ***6***, 34411-34421. (c) B. Aguila, Q. Sun, J. A. Perman, L. D. Earl, C. W. Abney, R. Elzein, R. Schlaf, S. Ma, *Adv. Funct. Mater.*, 2017, **26**, 1700665. DOI: 10.1002/adma.201700665.
15 K. Ai, C. Ruan, M. Shen, L. Lu, *Adv. Funct. Mater.*, 2016, **26**, 5542-5549.
16 (a) C. S. Diercks, Omar M. Yaghi, *Science*, **355**, 923; (b) R. P. Bisbey, W. D. Dichtel. *ACS Cent. Sci*., 2017, DOI: 10.1021/acscentsci.7b00127. (c) P. J. Waller, F. Gándara, O. M. Yaghi, *Acc. Chem. Res*. 2015, **48**, 3053-3063; (d) S. Y. Ding, W. Wang, *Chem. Soc. Rev*., 2013, **42**, 548-568; (e) J. W. Colson, W. R. Dichtel, *Nat. Chem.,* 2013, **5**, 453-465; (f) J. L. Segura, M. J. Mancheño; F. Zamora, *Chem. Soc. Rev.*, 2016, **45**, 5635- 5671; (g) N. Huang, P. Wang, D, Jiang, *Nat. Rev. Mater.*, 2016, **1**, 16068; (h) Y. Zhao, *Chem. Mater*., 2016, **28**, 8079-8081.
17 (a) H. Xu, J. Gao, D. Jiang, *Nat. Chem.* 2015, **7**, 905-912; (b) M. S. Lohse, T. D. Stassin, G. Naudin, S. Wuttke, R. Ameloot, D. De Vos, D. D. Medina, T. Bein, *Chem. Mat*., 2015, **28**, 626-631; (c) Bunck, D. N.; Dichtel, W. R. *Chem. Commun*., 2013, **49**, 2457-2459.
18 S. Y. Ding, M. Dong, Y. W. Wang, Y. T. Chen, H. Z. Wang, C. Y. Su, W. Wang, *J. Am. Chem. Soc.*, 2016, **138**, 3031-3037.
19 N. Huang, L. Zhai, H. Xu, D. Jiang, *J. Am. Chem. Soc.*, 2017, **139**, 2428-2434.
20 Q. Sun, B. Aguila, J. Perman, L. D. Earl, C. W. Abney, Y. Cheng, H. Wei, N. Nguyen, L. Wojtas, S. Ma, *J. Am. Chem. Soc.,* 2017, **139**, 2786-2793.
21 (a) A. Morsalia, M. Y. Masoomi, *Coord. Chem. Rev*., 2009, **253**, 1882-1905; (b) D. C. Bebout, *Mercury: Inorganic & Coordination Chemistry . In Encyclopedia of Inorganic and Bioinorganic Chemistry;* John Wiley & Sons, Ltd.: New York, 2011.

View Article Online
DOI: 10.1039/C7TA05588A

22 (a) J. G. Haasnoot, *Coord. Chem. Rev*., 2000, **200–202**, 131-185; (b) M. H. Klingele, S. Brooker, *Coord. Chem. Rev*., 2003, **241**, 119-132; (c) G. Aromí, L. A. Barrios, O. Roubeau. P. Gamez, *Coord. Chem. Rev.,* 2011, **255**, 485-546.
23 V. Castro, H. Rodríguez, F. Albericio, *ACS Comb. Sci*., 2016, **18**, 1-14.
24 Selected examples of triazole moieties as binders for Hg(II) can be found in: (a) J. Wong, N. Proschogo, M. Todd, P. J. Rutledge *Eur. J. Inorg. Chem*., 2017, 1075-1086; S. Areti, S. Bandaru, C. P. Rao, *ACS Omega* 2016, **1**, 626-635; (b) L. Li, C-F. Ke, H-Y. Zhang, Y. Liu, *J. Org. Chem*., 2010, **75**, 6673-6676.
25 E. Bermejo, A. Castiñeiras, I. García-Santos, R. Rodríguez-Riobó, *CrystEngComm*, 2016, **18**, 3428-3446.
26 P. Lian, H-B. Guo, D. Riccardi, A. Dong, J. M. Parks, Q. Xu, E. F. Pai, S. M. Miller, D-Q. Wei, J. C. Smith, H. Guo, *Biochemistry* 2014, **53**, 7211-7222.
27 Selected examples of sulphur functionalized materials: (a) Ref. 13; (b) G. Y. Oh, C. D. Morris, M. G. Kanatzidis, *J. Am. Chem. Soc.*, 2012, **134**, 14604-14608; (c) X. Feng, G. E. Fryxell, L. Q. Wang, A. Y. Kim, J. Liu, K. M. Kemner, *Science*, 1997, **276**, 923-926; (d) T. F. Baumann, J. G. Reynolds, *Chem. Commun*., 1998, 1637-1638; (e) Y. Shin, G. E. Fryxell, W. Um, K. Parker, S. V. Mattigod, R. Skaggs, *Adv. Funct. Mater.*, 2007, **17**, 2897-2901. (f) T. Hasell, D. J. Parker, H. A. Jones, T. McAllister, S. M. Howdle, *Chem. Commun*., 2016, **52**, 5383–5386.
28 S. Zhang, Y. Zhao, *J. Am. Chem. Soc.*, 2010, **132**, 10642-10644.
29 (a) X. B. Chen, X. D. Feng, J. Liu, G. E. Fryxell, M. L. Gong, *Sep. Sci. Technol*., 1999, **34**, 1121-1132; (b) W. Yantasee, C. L. Warner, T. Sangvanich, R. S. Addleman, T. G. Carter, R. J. Wiacek; G. E. Fryxell, C. Timchalk, M. G. Warner, *Environ. Sci. Technol.,* 2007, **41**, 5114-5119.
30 C. Q. Liu, Y. Q. Huang, N. Naismith, J. Economy, *Environ. Sci. Technol.*, 2003, **37**, 4261-4268.
31 (a) S. Bag, P. N. Trikalitis, P. J. Chupas, G. S. Armatas, M. G. Kanatzidis, *Science*, 2007, **317**, 490-493; (b) M. G. Kanatzidis, *Adv. Mater.*, 2007, **19**, 1165-1181.
32 (a) Ref. 27c; (b) J. Liu, X. D. Feng, G. E. Fryxell, L. Q. Wang, A. Y. Kim, M. L. Gong, *Adv. Mater*., 1998, **10**, 161-165; (c) Ref. 29a.
33 (a) S-Y. Ding, J. Gao, Q. Wang, Y. Zhang, W-G. Song, C-Y. Su, W. Wang, *J. Am. Chem. Soc*., 2011, **133**, 19816-19822; (b) D. Mullangi, S. Nandi, S. Shalini, S. Sreedhala, C. P. Vinod, R. Vaidhyanathan, *Sci. Rep*., 2015, **5**, 10876.
34 (a) Y. S. Ho, *J. Hazard. Mater.*, 2006, **136**, 681-689; (b) A. Farrukh, A. Akram, A. Ghaffar, S. Hanif, A. Hamid, H. Duran, B. Yameen, *ACS Appl. Mater. Interfaces*, 2013, **5**, 3784-3793. (c) Z. H. Fard, C. D. Malliakas, J. L. Mertz, M. G. Kanatzidis, *Chem. Mater.*, 2015, **27**, 1925-1928.
35 R. Qu, M. Wang, R. Song, C. Sun, Y. Zhang, X. Sun, C. Ji, C. Wang, P. Yin, *J. Chem. Eng. Data*, 2011, **56**, 1982-1990.
36 M. J. Manos, M. G. Kanatzidis, *Chem. Eur. J.* 2009, **15**, 4779-4784.
37 M. J. Manos, V. G. Petkov, M. G. Kanatzidis, *Adv. Funct. Mater,*. 2009, **19** , 1087-1092.
38 D. Saha, S. Barakat, S. V. Bramer, K. A. Nelson, D. K. Hensley, J. Chen, *ACS Appl. Mater. Interfaces*, 2016, **8**, 34132-34142.
39 Y. Busto, X. Cabrera, F.M.G. Tack, M.G. Verloo, *J. Hazard. Mater*. 2011, **186**, 114-118.
40 S. R. Bhatta, V. Bheemireddy, G. Vijaykumar, A. Thakura, *Sens. Actuators, B*, 2017, **240**, 640-650.

View Article Online
DOI: 10.1039/C7TA05588A

Graphical Abstract and TOC

An outstanding and selective material for Hg(II) polluted water remediation based on an imine-linked COF endowed with triazole and thiol groups.